Published in final edited form as:
Cancer Res. 2014 January 1; 74(1): 38–43. doi:10.1158/0008-5472.CAN-13-1981.

The NADH Oxidase ENOX1, a Critical Mediator of Endothelial Cell Radiosensitization, is Crucial for Vascular Development

Amudhan Venkateswaran[1], **Konjeti R. Sekhar**[1], **Daniel S. Levic**[2], **David B. Melville**[2], **Travis A Clark**[3], **Witold M. Rybski**[2], **Alexandra J. Walsh**[4], **Melissa C. Skala**[4], **Peter A. Crooks**[5], **Ela W. Knapik**[2,*], and **Michael L. Freeman**[1,*]

[1]Department of Radiation Oncology, Vanderbilt School of Engineering, Nashville, TN 37232

[2]Department of Medicine and Cell & Developmental Biology, Vanderbilt School of Engineering, Nashville, TN 37232

[3]Genomic Sciences Resources, Vanderbilt University Medical Center, Nashville, TN 37232

[4]Biomedical Engineering, Vanderbilt School of Engineering, Nashville, TN 37232

[5]School of Pharmacy, University of Arkansas for Medical Sciences, Little Rock, AR 72205

Abstract

ENOX1 is a highly conserved NADH oxidase that helps to regulate intracellular nicotinamide adenine dinucleotide levels in many cell types including endothelial cells. Pharmacological and RNAi-mediated suppression of ENOX1 impairs surrogate markers of tumor angiogenesis/vasculogenesis, providing support for the concept that ENOX1 represents an antiangiogenic druggable target. However, direct genetic evidence that demonstrates a role for ENOX1 in vascular development is lacking. In this study we exploited a zebrafish embryonic model of development to address this question. Whole mount *in situ* hybridization coupled with immunofluorescence performed on zebrafish embryos demonstrate that *enox1* message and translated protein are expressed in most tissues, and its expression is enriched in blood vessels and heart. Morpholino-mediated suppression of Enox1 in Tg(*fli1-eGFP)* and Tg(*flk1-eGFP)* zebrafish embryos significantly impairs the development of vasculature and blood circulation. Using i*n vivo* multiphoton microscopy, we show that morpholino-mediated knockdown of *enox1* increases NADH levels, consistent with loss of enzyme. VJ115 is a small molecule inhibitor of Enox1's oxidase activity shown to increase intracellular NADH in endothelial cells; we used VJ115 to determine if the oxidase activity was crucial for vascular development. We found that VJ115 suppressed vasculogenesis in Tg(*fli1-eGFP)* embryos and impaired circulation. Previously, it was shown that suppression of ENOX1 radiosensitizes proliferating tumor vasculature, a consequence of enhanced endothelial cell apoptosis. Thus our current findings, coupled with previous research, support the hypothesis that ENOX1 represents a potential cancer therapy target, one that combines molecular targeting with cytotoxic sensitization.

Keywords

ENOX1; NADH Oxidase; vasculogenesis; cancer

[*]*Corresponding Authors*: Ela W Knapik, MD 1165B Light Hall, Department of Medicine, Division of Genetic Medicine, Vanderbilt University School of Medicine, Nashville, TN 37232; Tel.: 615-322-7569; fax: 615-322-7549; ela.knapik@vanderbilt.edu Michael L Freeman, PhD, B 902 TVC Radiation Oncology, Vanderbilt University School of Medicine, Nashville, TN 37232; Tel.: 615-322-3606; fax: 615-343-3061; michael.freeman@vanderbilt.edu.

Conflicts of Interest: None

Introduction

Because of its critical role in promoting tumor growth, neovascularization represents a therapeutic pathway worthy of exploitation (1). However, targeting can be challenging because vascularization is not restricted to a single process. Tumors can utilize several processes, including sprouting angiogenesis, vasculogenesis, and/or vascular mimicry (2). This diversity of options may help to explain why current antiangeogenic monotherapy strategies can improve the duration of progression-free survival, but has not increased overall survival (3). Overcoming this problem requires a comprehensive understanding of the pathways that regulate vascularization.

Evolving research indicates that adaption of endothelial cell metabolism to the tumor microenvironment is a critical step in tumor vascularization (4). Proangiogenic tumor microenvironments can subject endothelial cells to conditions that require reprograming from respiration to glycolytic ATP production (4). Rapidly changing endothelial cell bioenergetic demands may require a switch to glutamine anaplerosis (4). These, as well as important ribosylation and deacetylation pathways (5), are driven by oxidized and reduced nicotinamide adenine dinucleotide cofactors (NAD^+ & NADH), whose levels are maintained by both redox recycling and biosynthesis. Failure to maintain nicotinamide adenine dinucleotide homeostasis can impair ATP production, polyADP ribosylation, and NAD^+ -dependent deacetylation. Although poorly understood, NAD^+ has been shown to promote endothelial cell migration (6) while the nicotinamide adenine dinucleotide biosynthetic inhibitor FK866/K22.175 has been found to be antiangiogenic (7). Thus, one can conceptualize that nicotinamide adenine dinucleotide cofactors support vasculogenesis and angiogenesis (5), two important processes that contribute to tumor neovascularization.

ENOX1 is a NADH oxidase that regulates nicotinamide adenine dinucleotide homeostasis through oxidization of NADH to NAD^+ (8). The gene is highly conserved in vertebrates (98% identity between *H. sapiens* and *M. musculus*; 72% identity between *H. sapiens* and *D. rerio*). Purified enzyme exhibits NADH oxidase and protein disulfide-thiol interchange activity, with a periodicity of 24 min (9). However, we have only been able to validate the presence of the oxidase activity *in vivo* (10). The enzyme resides at the ecto-surface of the plasma membrane. Differential detergent fractionation studies reveal that ENOX1 is also present in the cytoskeletal compartment of endothelial cells (unpublished data). RNAi-mediated suppression of ENOX1 in human or mouse endothelial cells inhibits migration and the ability to form tubule-like structures in matrigel (11). VJ115 is a (Z)-(+/−)-2-(1-benzylindol-3-ylmethylene)-1-azabicyclo[2.2.2]octan-3-ol that inhibits ENOX1's NADH oxidase activity and therefore significantly increases intracellular NADH (10, 11). VJ115 inhibits formation of tubule-like structures by endothelial cells in matrigel and tumor cell-mediated neo-angiogenesis, as assessed in a dorsal skinfold vascular window model (11). Administration of daily injections of VJ115 to mice with syngeneic Lewis Lung Carcinoma xenografts produces the same degree of tumor growth delay as fractionated x-irradiation (11). We thus reasoned that ENOX1 represents a potential druggable target for the inhibition of angiogenesis/vasculogenesis.

Zebrafish embryos represent a transparent and genetically tractable model for the study of angiogenesis and vasculogenesis. The dorsal aorta and posterior cardinal vein are first formed by vasculogenesis. Then secondary vessels, such as intersegmental vessels, are formed by classical sprouting angiogenesis (2). Herein we used two transgenic zebrafish embryonic models: Tg(*fli-1:eGFP*) and Tg(*flk1:eGF*) to establish a role for ENOX1 in vascularization. We then demonstrate that pharmacological targeting of the oxidase inhibits vascularization and blood flow.

Materials and Methods

Zebrafish Stocks and Growth Conditions

Zebrafish strains AB, *Tg(fli1:eGFP)* and *Tg(flk1:eGFP)* were raised in Vanderbilt's Zebrafish facility. Briefly, all fish were grown at 28°C under standard conditions according to the policies and procedures of the Institutional Animal Care and Use Committee of Vanderbilt University Medical Center.

Morpholinos

Morpholino phosphorodiamidate oligonucleotides that targeted 2 separate intron-exon boundary sequences of *enox1* were designed by Gene Tools (Carvalis, OR). The sequences were as follows: MO1, 5'-AGATCTGCGCAATCCACAAAAATGC-3' and MO2, 5'-TAATCTGCTCAACTTTGGTGGGTAA-3'. Gene tools control non-silencing morpholino sequence was 5'-CCTCTTACCTCAGTACAATTTATA-3'. Morpholinos were dissolved in distilled water and 4 ng was injected into 1-cell stage embryos. Injection of control morpholinos did not produce a phenotype when compared to uninjected embryos (data not shown).

In vivo Multiphoton Microscopy of NADH

Microscopy was performed as described previously (12). A custom built, commercial multi-photon fluorescence microscope (Prairie Technologies) was used to acquire auto fluorescence images of NADH with a 40x water-immersion objective (1.15 NA). A titanium:sapphire laser (Coherent Inc.) provided excitation light at 750 nm with an average power at the sample of 7.5–7.8 mW. A GaAsP PMT (H7422P-40, Hamamatsu) was used to detect emitted photons through a 400–480 nm bandpass filter. A pixel dwell time of 4.8 μs was used for scanning each 256×256 pixel image. Each image was captured and averaged 8 times to reduce noise. For analysis, NADH fluorescence images were set to a threshold to remove background and nuclear fluorescence. The average NADH fluorescence intensity per cell was computed with ImageJ software.

Whole-Mount In Situ Hybridization

Wild-type embryos were grown to the desired developmental stage in 0.2 mM phenylthiourea in order to inhibit pigmentation. The embryos were fixed overnight in 4% paraformaldehyde (PFA) followed by dehydration in increasing concentrations of methanol, stage dependent treatment with proteinase K and hybridization with Dig-labeled enox1 antisense RNA probe. Antisense probes were generated with T7 RNA polymerase from a *Hind*III-linearized vector (Openbiosystems, clone id.: EXELIXIS3853870) containing a ~700 bp fragment of enox1.

Enox1 Antibody

In collaboration with the Vanderbilt Antibody Core and Covance Inc., (Denver, PA), a custom ENOX1 antibody was raised by injecting rabbits with antigen conjugated with ENOX1 specific peptide [H]-CKEEQSHTQALLKVLQEQLKGTK-[NH2] (10).

Immunofluorescence

Embryos were fixed in 4% PFA at 4°C overnight and then treated in 30% sucrose at 4°C followed by embedding in OCT medium and sectioning. Zebrafish cryosections were incubated with 1:300 diluted primary antibody against Enox1 followed by 1:300 Alexa Fluor 555 fluorescently conjugated secondary antibody (Molecular Probes). DAPI was used for nuclear counterstaining. Confocal images were taken with an Olympus FV-1000 inverted confocal microscope (Vanderbilt Cell Imaging Shared Resource).

Quantitative RT-PCR

Total RNA was extracted from 50 embryos at different embryonic developmental stages and cDNA synthesis and real-time PCR using SYBER-Green Supermix (Biorad) was performed. The following primers were used to amplify *enox1*: F, 5'-TTGGGGTCCTTTGAGATCAG-3' and R, 5'GGCAGTCGCACCATTAATCT-3'. All experiments were performed in triplicate.

Western Blotting

Embryos at different developmental stages were deyolked by scraping them off using a sterile syringe and cell lysates were obtained using RIPA buffer containing protease inhibitor (Sigma). The egg yolk was removed before homogenization. Protein concentration was measured using Biorad protein assay reagent. Standard western blotting protocol was followed using Enox1 antibody. Twenty-five embryos were used for protein extraction for each time point.

Methods for FACS and RNA Seq library preparation, sequencing, and transcriptome analysis are available as Supplementary Methods on line.

Results and Discussion

We generated an antibody to ENOX1 (10) that detects human ENOX1, murine Enox1, and zebrafish Enox1, whereas preimmune sera does not (Supplementary Figs 1A and 1B). The ability to detect human ENOX1 using the ENOX1 antibody was validated using ENOX1 shRNA (Supplementary Fig 1C). Morpholinos (MO), designed against two different regions in the *enox1* gene and injected at the 1-cell stage significantly suppressed expression of *enox1* mRNA, as determined by qRT-PCR performed 48 hours post fertilization (hpf) ($P < 0.005$, Student's t-test). Immunoblotting validated morpholino-mediated suppression of zebrafish Enox1. Representative data are shown in Supplementary Figs 1D and 1E.

We evaluated Enox1 expression in zebrafish embryos. Whole-mount *in-situ* hybridization using an *enox1* antisense RNA probe to exons 1–6 revealed expression of *enox1* mRNA in longitudinal axial vessels (i.e. dorsal aorta/posterior cardinal vein) 24 hours hpf and in heart 48 hpf (Fig. 1A and 1B). Confocal immunofluorescent imaging of Enox1 72 hpf revealed expression of Enox1 in a number of tissues (Fig 1C), including heart (Fig 1C), tail and chondrocytes (Supplementary Fig S2).

The transcription factor *fli1* is one of the earliest and well-validated indicators of vasculature development (13). We made a single cell suspension from 24 hpf *Tg*(*Fli1:GFP*) embryos, immunostained the cells with Enox1 antibody and quantified the number of cells that expressed both eGFP and Enox1immunofluoresence by FACS. The analysis indicated that more than 90% of Fli1-GFP expressing cells co-expressed Enox1 (Fig 1D).

We used multiphoton fluorescence microscopy, which records intrinsic NADH fluorescence intensity in live cells (12), to determine NADH levels (Fig. 2). Whole-mount *in-situ* hybridization (Fig 1), RT-PCR, and immunoblotting (data not shown) established that Enox1 was expressed 24 hpf, a time where optical clarity is excellent. Two areas in each embryo's tail were analyzed. Suppression of Enox1 was accompanied by increased NADH levels in *enox1* morphants compared to control ($P < 0.05$, Rank Sum test, Fig. 2B), a result that can be attributed to loss of Enox1 oxidase activity.

Whole-transcriptome sequencing of 20 *enox1* morphant and 20 control embryos was undertaken at 48 hpf. Expression of 867 transcripts in *enox1* morphants exhibited a $\log_2$ <-1.0 or > 1.0-fold change ($P < 0.05$, cut-off at 5% false discovery rate as a threshold,

Supplementary Dataset 1). The PANTHER 8.1 classification system (14) mapped 549 of the 608 down-regulated transcripts; 43% (236) were assigned to GO:0008152, metabolic processing (Supplementary Dataset S2). Of the 259 up-regulated transcripts, 224 were mapped and 53% (119) were assigned to GO:0008152 (Supplementary Dataset S3). This analysis suggests that Enox1 activity supports metabolic processes.

As the transcription factor *Fli1* is a well characterized endothelial marker (15), we examined *fli-1* promoter-driven eGFP vascular expression in control, MO1, and MO2 *Tg*(*fli1:eGFP*) embryos. Seventy five percent of morphants did not express discernible eGFP expression ($P < 0.001$, Fisher's exact test, see Fig 3A for example). The remaining 25% of the *enox1* morphants exhibited a partial loss of vasculature, defined as embryos that expressed longitudinal axial vessels but failed to develop intersegmental arteries and veins (see Supplementary Fig 3A and supplementary videos for example). The zebrafish *flk-1* gene encodes a receptor tyrosine kinase that was used as second marker of vasculogenesis. Examination of *flk-1* promoter-driven eGFP vascular expression at 48 hpf in control and *enox1Tg*(*flk1:eGFP*) morphants indicated that 45% of the morphants did not have discernible eGFP expression ($P < 0.001$, Fisher's exact test). The remainder exhibited a partial loss, as defined above (Fig 3B). Nomarski Interference contrast microscopy was used to assess morphology (Supplementary Fig 3B). The presence of ISV in control embryos (blue arrows) is diminished in *enox1* morphants (red arrow). DIC images illustrate the presence of pericardial oedema, a finding that is consistent with the morphological defects found in VEGF-A morphant zebrafish (15). These data and previous research which demonstrated that Enox1 shRNA suppressed mammalian endothelial cell proliferation and migration (11) suggest that Enox1 plays a critical role in vasculature development. However, Enox1 is expressed in multiple tissues and the morpholinos are not endothelial-specific. Thus, we cannot rule out a role for Enox1-mediated paracrine signaling.

Video microscopy was used to obtain further evidence that Enox1 is crucial for vascular function. Movies comparing circulation in trunk/tail of control and *enox1* morphants are provided as Supplementary Video S1 & S2 and demonstrate significant reduction in circulation in enox1 depleted animals.

Expression of transcription factors and membrane receptors critical for vascular development (16), such as *etvc*, *gata2a*, *fli1a*, *flka*, or *flkb* were not affected by loss of Enox1 ($P < 0.05$, Supplementary Dataset 4). However, the PANTHER analysis indicated that reprograming in *enox1* morphants resulted in up-regulation of the antiproliferation gene ENSDARG00000076554, p21/Cip1/Waf1 (increased 8.2-fold, $P < 3\times10^{-5}$) and the antiangiogenic protein ENSDARG00000056795, PAI-1 (increased 4.67-fold, $P = 0.0015$ (17)), as well as repression of proangiogenic proteins ENSDARG00000033655, Stathmin (decreased 5.8 fold, $P = 0.028$ (18)) and ENSDARG00000060597, Phosphatidylinositol-3-kinase (decreased 4-fold, $P = 0.0064$ (19), Supplementary Dataset 1. Although the exact mechanism by which Enox1 contributes to vasculogenesis is not yet known, the Panther analysis suggests the hypothesis that suppression of Enox1 impacts multiple pathways, which in aggregate impair vasculogenesis and angiogenesis.

VJ115 is a small molecule inhibitor of ENOX1's NADH oxidase activity. The compound produces significant radiation sensitization of Lewis Lung carcinoma (LLC) and HT29 xenografts (11). VJ115 also inhibits LLC-induced neoangiogenesis in a mouse window model (11) and phenocopies ENOX1 RNAi effects with regard to inhibiting HUVEC migration and inhibiting formation of tubule-like structures in Matrigel (11). Proteomic profiling revealed that exposure of HUVECs to VJ115 suppressed expression of STATHMIN (10). Thus, we determined if VJ115 could inhibit vascular development in *Tg*(*fli1:eGFP*) embryos. Embryos were exposed to either solvent control or 50 μM VJ115 at

the 18 somite stage. Expression of eGFP was examined 72 hpf. Eighty percent of VJ115-treated embryos failed to express eGFP ($P < 0.001$, Fisher's exact test, Fig 4). The remaining 20% of the embryos had a partial loss of eGFP expression, which may be a consequence of VJ115's poor water solubility. Compared to solvent control, we observed a lack of circulation in VJ115-treated embryos (Supplementary Videos S3 and S4). While we cannot rule out off target effects, these data strongly suggest that pharmacological targeting of Enox1 inhibits vascularization and circulation and that Enox1 is a targetable enzyme that is crucial for vascular development.

Analysis of cell-based functional assays coupled with either small molecule or RNAi methodology has demonstrated that radiation sensitivity is enhanced significantly by inhibition/suppression of ENOX1 in human and murine endothelial cells (11). Therefore we asked whether radiation sensitivity of zebrafish embryos could be impacted by loss of Enox1 activity. Whereas exposure of 24 hpf embryos to 0, 5, 10, 15 or 20 Gy of Cs137 gamma rays did not affect the ability of the embryos to hatch between 48 and 72 hpf ($P > 0.05$ ANOVA), exposure to 50 μM VJ115 30 min prior to irradiation resulted in a dose-dependent inhibition of hatching ($P = 0.0007$, n = 400, data not shown). For example, at 20 Gy VJ115 reduced hatching by 62.5%. Thus, VJ115-mediated inhibition of Enox1 activity radiosensitized zebrafish, similar to mammalian models.

An important paradigm that emerges from review of current cancer therapy clinical trials (20) is that the efficacy of antiangiogenic agents can be significantly enhanced by the addition of cytotoxic therapy, such as ionizing radiation. We have shown previously that genetic and pharmacological inhibition of ENOX1 produces significant radiosensitization of dividing endothelial cells, a consequence of caspase-mediated apoptosis. Non-proliferating endothelial cells were not radiosensitized (11). We have also shown that pharmacological targeting of ENOX1 significantly enhances radiation-mediated control of tumor vasculature, without producing overt toxicity in mice (11). Thus, our previous and current work supports an innovative concept that posits that ENOX1 represents a potential cancer therapy target, one that combines molecular targeting with cytotoxic sensitization.

Supplementary Material

Refer to Web version on PubMed Central for supplementary material.

Acknowledgments

We thank Melissa Stauffer of Scientific Editing Solutions for editing the manuscript and Dr. Penthala Narsimha for the synthesis of VJ115. It is with great pleasure that we thank Dr. Joshua T. Gamse, Vanderbilt University, for providing embryos, technical advice, and interpretation of data.

Financial Support: This work was supported in part by grants from the US National Institutes of Health/National Cancer Institute grants RO1CA140409 and T32CA093240 (M.L.F.), NIH NIDCR grant R01 DE018477 (E.W.K.), and the Vanderbilt-Ingram Cancer Center (grant P30 CA68485). The graduate students were supported by NICHD T32 HD007502-14 Vanderbilt University, Training Program in Developmental Biology, F31DE022226 (D.S.L.), and NIGMS T32 GM008554, the Cellular, Biochemical and Molecular Sciences Training Program at Vanderbilt (D.B.M).

References

1. Folkman J, Hanahan D. Switch to the angiogenic phenotype during tumorigenesis. Princess Takamatsu Symp. 1991; 22:339–47. [PubMed: 1726933]
2. Weis SM, Cheresh DA. Tumor angiogenesis: molecular pathways and therapeutic targets. Nat Med. 2011; 17:1359–70. [PubMed: 22064426]

3. Bottsford-Miller JN, Coleman RL, Sood AK. Resistance and escape from antiangiogenesis therapy: clinical implications and future strategies. J Clin Oncol. 2012; 30:4026–34. pmcid,3488272. [PubMed: 23008289]
4. Polet F, Feron O. Endothelial cell metabolism and tumour angiogenesis: glucose and glutamine as essential fuels and lactate as the driving force. J Intern Med. 2013; 273:156–65. [PubMed: 23216817]
5. Chiarugi A, Dolle C, Felici R, Ziegler M. The NAD metabolome--a key determinant of cancer cell biology. Nat Rev Cancer. 2012; 12:741–52. [PubMed: 23018234]
6. Murray B, Wilson DJ. A study of metabolites as intermediate effectors in angiogenesis. Angiogenesis. 2001; 4:71–7. [PubMed: 11824381]
7. Drevs J, Loser R, Rattel B, Esser N. Antiangiogenic potency of FK866/K22.175, a new inhibitor of intracellular NAD biosynthesis, in murine renal cell carcinoma. Anticancer Res. 2003; 23:4853–8. [PubMed: 14981935]
8. Herst PM, Berridge MV. Cell surface oxygen consumption: a major contributor to cellular oxygen consumption in glycolytic cancer cell lines. Biochim Biophys Acta. 2007; 1767:170–7. [PubMed: 17266920]
9. Morre DM, Lenaz G, Morre DJ. Surface oxidase and oxidative stress propagation in aging. J Exp Biol. 2000; 203:1513–21. [PubMed: 10769214]
10. Venkateswaran A, Friedman DB, Walsh AJ, Skala MC, Sasi S, Rachakonda G, et al. The novel antiangiogenic VJ115 inhibits the NADH oxidase ENOX1 and cytoskeleton-remodeling proteins. Invest New Drugs. 2013; 31:535–44. pmcid,3553230. [PubMed: 23054211]
11. Geng L, Rachakonda G, Morre DJ, Morre DM, Crooks PA, Sonar VN, et al. Indolylquinuclidinols inhibit ENOX activity and endothelial cell morphogenesis while enhancing radiation-mediated control of tumor vasculature. FASEB J. 2009; 23:2986–95. [PubMed: 19395476]
12. Skala MC, Riching KM, Gendron-Fitzpatrick A, Eickhoff J, Eliceiri KW, White JG, et al. In vivo multiphoton microscopy of NADH and FAD redox states, fluorescence lifetimes, and cellular morphology in precancerous epithelia. Proc Natl Acad Sci U S A. 2007; 104:19494–9. pmcid, 2148317. [PubMed: 18042710]
13. Brown LA, Rodaway AR, Schilling TF, Jowett T, Ingham PW, Patient RK, et al. Insights into early vasculogenesis revealed by expression of the ETS-domain transcription factor Fli-1 in wild-type and mutant zebrafish embryos. Mech Dev. 2000; 90:237–52. [PubMed: 10640707]
14. Thomas PD, Kejariwal A, Campbell MJ, Mi H, Diemer K, Guo N, et al. PANTHER: a browsable database of gene products organized by biological function, using curated protein family and subfamily classification. Nucleic Acids Res. 2003; 31:334–41. pmcid,165562. [PubMed: 12520017]
15. Nasevicius A, Larson J, Ekker SC. Distinct requirements for zebrafish angiogenesis revealed by a VEGF-A morphant. Yeast. 2000; 17:294–301. pmcid,2448381. [PubMed: 11119306]
16. De Val S. Key transcriptional regulators of early vascular development. Arterioscler Thromb Vasc Biol. 2011; 31:1469–75. [PubMed: 21677289]
17. Ebrahimian TG, Squiban C, Roque T, Lugo-Martinez H, Hneino M, Buard V, et al. Plasminogen activator inhibitor-1 controls bone marrow-derived cells therapeutic effect through MMP9 signaling: role in physiological and pathological wound healing. Stem Cells. 2012; 30:1436–46. [PubMed: 22570200]
18. Iancu-Rubin C, Atweh GF. p27(Kip1) and stathmin share the stage for the first time. Trends Cell Biol. 2005; 15:346–8. [PubMed: 15951178]
19. Choorapoikayil S, Weijts B, Kers R, de Bruin A, den Hertog J. Loss of Pten promotes angiogenesis and enhanced vegfaa expression in zebrafish. Dis Model Mech. 2013
20. Jayson GC, Hicklin DJ, Ellis LM. Antiangiogenic therapy--evolving view based on clinical trial results. Nat Rev Clin Oncol. 2012; 9:297–303. [PubMed: 22330688]

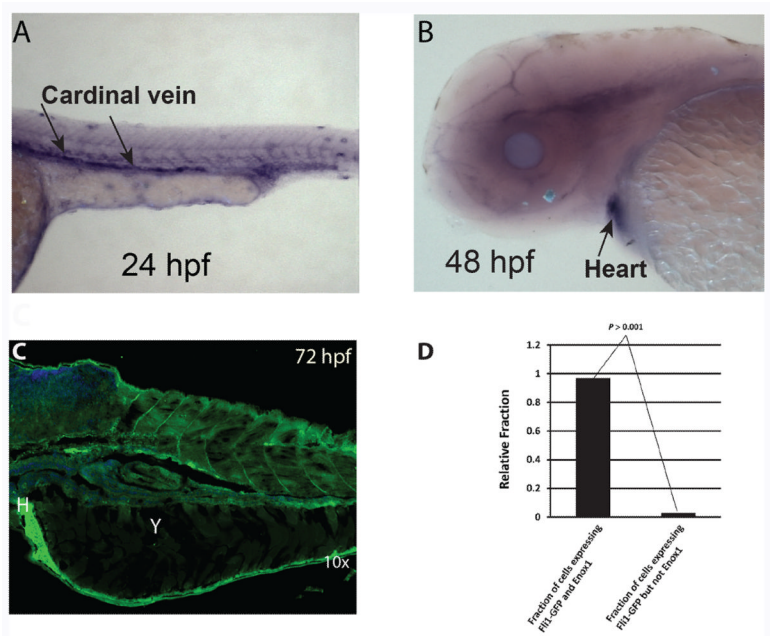

Figure 1.

Expression of Enox1 in zebrafish embryos. A) *In situ* hybridization of *enox1* antisense probe at the longitudinal axial vessels (A) and heart (B). C) Confocal imaging of Enox1 Alexa 488 green at 72 hpf. Y = yolk, H = Heart; D) Singe cell suspensions of 24 hpf *Tg(Fli1:GFP)* embryonic cells analyzed by FACS for GFP fluorescence and/or Enox1 Rhodamine Red immunofluorescence.

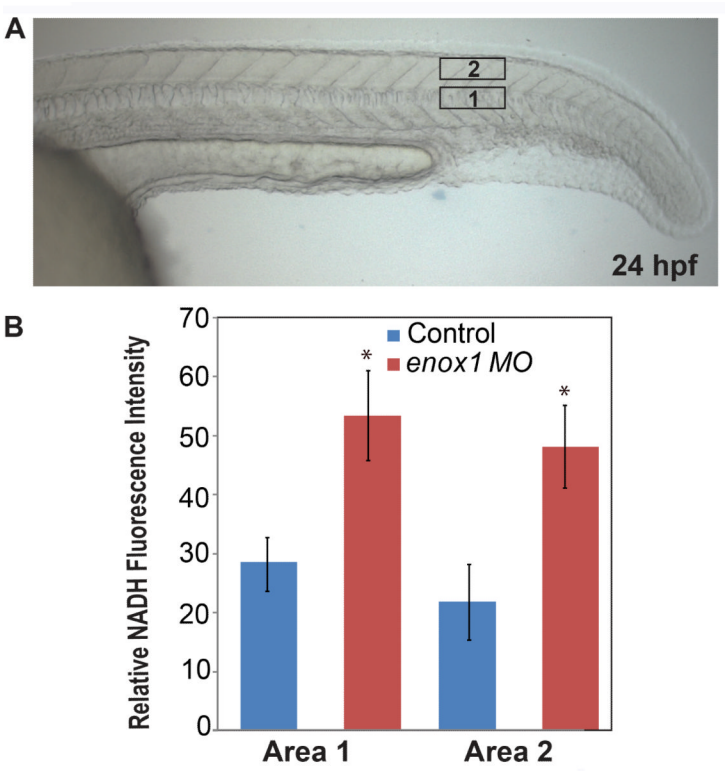

Figure 2.
Intracellular NADH is increased in enox1 morphants compared to control embryos. (A) Representative Nomarski interference contrast microscopy image of 24 hpf zebrafish embryo. Two areas of interest are noted. (B) *In vivo* multiphoton microscopy was used to measure NADH fluorescence at a depth of 20 microns in area 1 and 2 (n=6 embryos, 3 fields per embryo). * $P < 0.05$

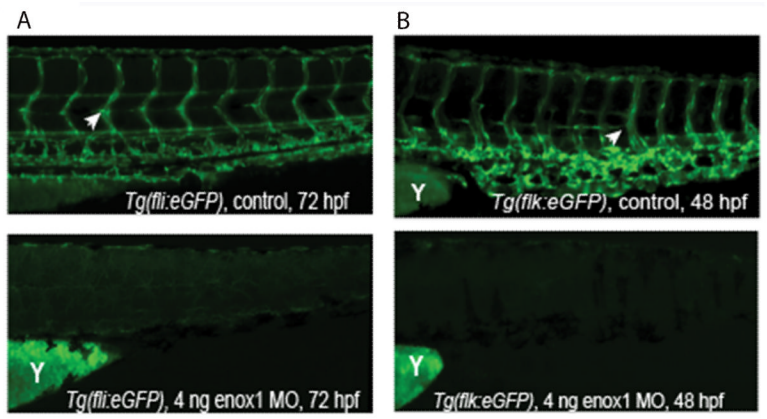

Figure 3.

Loss of fl1i- or flk1 promoter-driven eGFP vascular expression in *enox1* morphants. (A) Vascular eGFP expression at 72 hpf in control (n = 201) or *enox1* morphant (MO1, n = 207) *Tg(fli1:eGFP)* embryos; B) Vascular eGFP expression at 48 hpf in control (n = 201) or *enox1* morphant (MO1, n = 209) *Tg(flk1:eGFP)* embryos. Yolk is denoted by the letter `Y'. White arrowheads indicate expression of eGFP in ISVs.

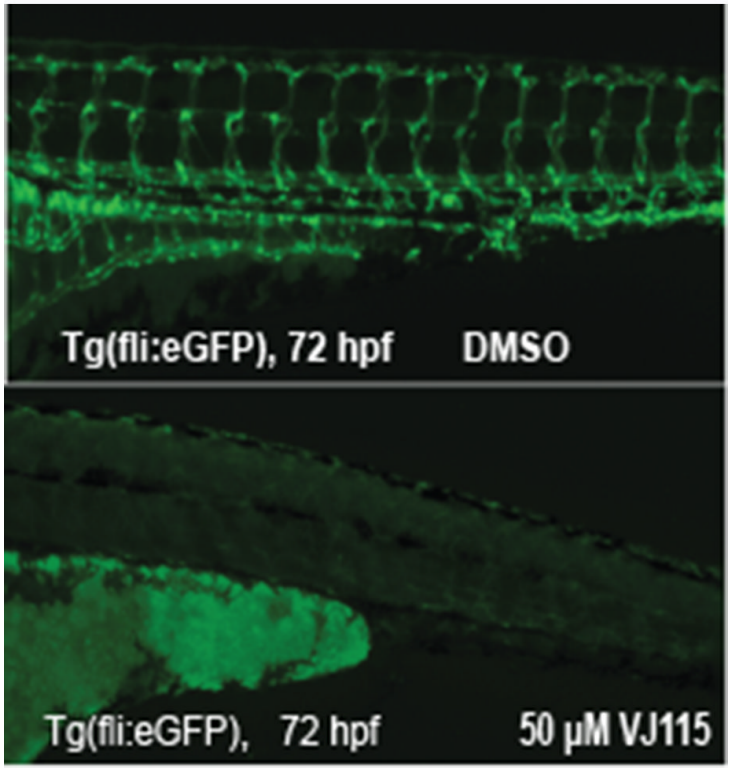

Figure 4.
VJ 115 inhibits vasculogenesis in *Tg(fli1:eGFP)* embryos. *Tg(fli:eGFP)* embryos were exposed to solvent control (DMSO, n = 201) or 50 μM VJ115 (n = 204) from an 18 somite stage until evaluation at 72 hpf.